CONTRIBUTION OF LOW-FREQUENCY RAMAN SPECTROSCOPY TO DETERMINE THE SOLUBILITY CURVES OF DRUGS IN POLYMERS: THE CASE OF PARACETAMOL / PVP

Mansour Latreche, Jean-François Willart*, Laurent Paccou, Yannick Guinet,

Florence Danède and Alain Hédoux

Univ. Lille, CNRS, INRAE, ENSCL, UMR 8207
UMET - Unité Matériaux et Transformations, F-59000 Lille, France

Abstract:

A new method for determining solubility lines of drugs in polymers, based on low-frequency Raman spectroscopy measurements, is described and the results obtained by this method are compared with those obtained using a more classical method based on differential scanning calorimetry investigations. This method was applied to the paracetamol / PVP system using molecular and crystalline dispersions (MCD) rather than usual physical mixtures to reach faster the equilibrium saturated states and make the determination of the solubility line more rapid.

* Corresponding author: Jean-Francois.Willart@univ-lille.fr

Keywords : Low-Frequency Raman Spectroscopy – Molecular and Crystalline Dispersions – Physical stability – poorly soluble drugs

1. INTRODUCTION

Improving the solubility of the more and more numerous poorly soluble drugs is an actual challenge of the pharmaceutical research[1-4]. In this context, amorphous solid dispersions[1-6] of drugs into polymers are recognized to be promising systems to reach this goal for two main reasons: (i) Amorphous drugs have better dissolution properties – more properly dilution properties – than their crystalline counterparts[7-9]. (ii) The molecular dispersion of the drug in the polymer prevents its recrystallization which is generally unavoidable in the pure bulk amorphous state[10-13]. However, this last point requires that the drug concentration does not exceed the solubility limit of the drug into the polymer. It thus appears that the determination of the solubility line of the drug in the polymer is of prime interest to determine the maximum amount of drug which can be loaded without a risk of recrystallization at a given temperature[14-19].

Several experimental techniques have already been proposed to determine the solubility line of drug / polymer systems. However, most of them require to dissolve the drug into the polymer during the heating – or the annealing – of a physical mixture of the two components. This results generally in a very slow dissolution process due to the usually high viscosity of polymers. Reaching equilibrium saturated states thus becomes increasingly difficult on approaching the glass transition temperature (Tg) of the polymer and appears to be impossible, in practice, below Tg. Recently, Latreche et al.[20] have shown that much faster dissolution rates could be obtained by using Molecular and Crystalline Dispersions (MCD) instead of physical mixtures. MCD can be easily obtained, directly in the solid state, in two steps. In the first step a glass solution is produced by co-milling the drug and the polymer. In the second stage, this glass solution is annealed for a few hours in a plasticizing atmosphere (typically ethanol) to involve a strong but partial recrystallization of the drug, and then dried. In these systems, the drug is thus dispersed in the polymer partly at the molecular level and partly in the form of a myriad of small crystallites. Such a microstructure strongly improves the dissolution rate of the crystalline faction in the polymer for two reasons: The molecular dispersion induces a plasticization which increases the molecular mobility in the solution, while the fine dispersion of crystalline grains strongly reduces the diffusion length required for the drug molecules to invade homogeneously the polymer. Moreover, since the crystallites arise from a crystallization process, their specific dispersion (size and spatial repartition) is expected to be that which best facilitates the inverse process of (re)dissolution of the crystallites.

In this paper, we show how to use LFRS (Low-Frequency Raman Spectroscopy) to determine the solubility line of a drug in a polymer during the heating of a MCD of the two components. A special attention will be given to the capability of LFRS to directly determine the fraction of drug dissolved inside the polymer[20], allowing a direct and fast determination of the solubility line in the course of a single heating experiment. The demonstration will be performed with the paracetamol / PVP binary mixture. The validity of the method will then be evaluated by comparing the solubility line derived from LFRS measurements to that obtained from conventional DSC investigations.

2. MATERIALS AND METHOD

Cryogenic milling was performed in a vibrating CryoMill (Retsch). We used ZrO_2 milling jar of 25 cm^3 with 1 ball (Ø = 15 mm) of the same material. 0.5 g of material was placed in the mill. The vibration frequency was set to 30 Hz and milling periods (10 min) were alternated with pause periods (5 min) to limit the mechanical heating of the sample.

Annealing under ethanol atmosphere was performed at room temperature (RT) by placing samples into a desiccator containing liquid ethanol.

Powder X-ray diffraction (PXRD) experiments were performed with an XPERT PRO MPD diffractometer ($\lambda_{CuK\alpha}$ = 1.540 Å) equipped with an X'celerator detector. Samples were placed into Lindemann glass capillaries (Ø = 0.7mm). All measurements were performed at RT.

Differential Scanning Calorimetry (DSC) experiments were performed with a Discovery micro calorimeter of TA Instruments. During all the measurements the calorimeter head was flushed with highly pure nitrogen gas. Temperature and enthalpy readings were calibrated using pure indium at the same scan rates used in the experiments. All DSC scans were performed at the rate of 5°C / min. The samples have been placed in open pans (pans with no lid) in order to allow any water absorbed during processing to evaporate upon heating. Small sample sizes (typically 4 mg) were used to achieve a good resolution and a good thermal conductivity.

Low-frequency Raman spectroscopy (LFRS) experiments were performed using a high-dispersive spectrometer (XY Dilor) composed of three gratings, four mirrors organized with respect to the detector in a configuration characterized by a focal length of 800 mm. The choice of experimental conditions (incident radiation, entrance and exit slit width opened at 150 µm) gives a spectral resolution of about 1 cm^{-1} in the 5 – 200 cm^{-1} region, and allows the rejection of exciting light (the 647.1 nm line of a mixed argon-krypton Coherent laser) down to 5 cm^{-1}. The spectrometer is equipped with a liquid nitrogen cooled charge coupled device detector. The high sensitivity of the detector and the large analyzed scattered volume (~ 0.5 cm^3) allow to record low-frequency Raman spectra in the 5 – 200 cm^{-1} range in 120 seconds. Powder samples were loaded in spherical pyrex cells hermetically sealed. The temperature of sample was regulated using an Oxford nitrogen flux device that keeps temperature fluctuations within 0.1°C.

Crystalline Paracetamol ($C_8H_9NO_2$) was provided by SIGMA ALDRICH® and used without any further purification.

Amorphous **PVP K12 PF** (M_w = 2000-3000 $g.mol^{-1}$, 5% w/w moisture) was kindly provided by BASF and was used without any further purification

Molecular / Crystalline Dispersions (MCD) of paracetamol and PVP were produced using a two-stage protocol which was previously described in details in reference [20]. During the first stage, a physical mixture paracetamol / PVP [85:15] was cryo-milled during 1 hour. The

diffractograms of this mixture recorded before and after cryo-milling are reported in figure 1. Before milling the diffractogram shows Bragg peaks characteristic of the crystalline form I of paracetamol, while after milling these Bragg peaks have almost disappeared. This indicates that the two compounds have been co-amorphized during the milling process. During the second stage, the milled sample has been annealed for two hours at 20°C, under a plasticizing ethanol atmosphere. It was then dried by annealing at 80°C for 1 hour. The absence of ethanol in the dried sample was checked through a TGA scan (5°C / min) which does not show any loss of mass associated with the departure of this plasticizer. Figure 1 shows the diffractogram of the dried sample. It shows many Bragg peaks characteristic of form I which indicates that a large part of paracetamol has recrystallized toward the initial crystalline form during the annealing under ethanol atmosphere. The overall protocol thus gives rise to a MCD where paracetamol is dispersed into the PVP matrix both at the molecular level and in the form of small crystalline grains.

Glass solutions paracetamol / PVP were produced by melting (5°C / min) and quenching (20°C / min) in the DSC device, physical mixtures of the two components. Different compositions varying from pure paracetamol to pure PVP were investigated. The evolution of Tg with composition (Gordon Taylor curve) was determined by rescanning (5°C / min) the different glass solutions. The results are reported in figure 3 together with the best fit of the usual Gordon Taylor law[21] to the data. This curve will be used as a calibration curve to determine the solubility line of paracetamol in PVP in section 3.1.

3. RESULTS AND DISCUSSION

3.1 Determination of the solubility curve by DSC

The solubility curve of paracetamol in PVP was determined by DSC through the repetition of the 3-step thermal treatment schematically shown in figure 2:

(i) In the first step, the MCD is annealed at some temperature T_a for 1 hour. During this stage, the crystalline fraction of paracetamol dissolves into the polymer matrix to reach the saturated state at this temperature. The annealed sample is thus made of crystalline grains of paracetamol embedded into a glass solution paracetamol / PVP having a paracetamol concentration corresponding to the equilibrium saturation at T_a.

(ii) In the second step, the sample was rapidly cooled down by removing the sample from the DSC and placing it on a cold plate at -20°C. This fast cooling was used to avoid any recrystallization of paracetamol dissolved in the polymer matrix which happens to be supersaturated below T_a.

(iii) In the third step, the sample is rescanned (5°C / min) to determine the glass transition temperature of the glass solution paracetamol / PVP. Using the Gordon Taylor plot of the binary mixture as a calibration curve (figure 3), the Tg of the glass solution gives directly access to its paracetamol concentration. This concentration associated with the previous annealing temperature T_a thus gives one point of the solubility curve.

To determine the next points of the solubility curve, the last DSC scan is performed up to a slightly higher annealing temperature (T_a) where steps i, ii and iii are repeated. The points of the solubility curve thus obtained are reported in figure 3.

3.2 Determination of the solubility line by Low Frequency Raman Spectroscopy (LFRS)

We show here how to use LFRS to determine the solubility line of a drug in a polymer. The method consists to follow the evolution of the structural composition of a MCD in the course of a heating treatment.

(i) Data processing of LFRS in disordered materials[22,23]

The procedure for determining the structural composition of a MCD by LFRS is based on the method previously used for determining the crystalline fraction during the crystallization process of an amorphous molecular material. This method requires a data preprocessing specific to the low-frequency Raman spectrum (LFRS) of disordered molecular materials previously described in references [22,23] and summarized below. In a first step, Raman intensity is transformed into reduced intensity $I_r(\omega)$, using[24]:

$$I_r(\omega) = \frac{I_{Raman}(\omega,T)}{[n(\omega,T)+1]\omega} \qquad (1)$$

to provide the Raman band shape free of temperature fluctuations, where $n(\omega,T)$ is the Bose-Einstein factor. Figure 4a shows the spectra of amorphous paracetamol recorded in the glassy state (-20°C) and in the undercooled liquid state (120°C), plotted in reduced intensity. They show the typical band-shape of the LFRS of a disordered molecular material, strongly temperature dependent and dominated by the low-frequency quasielastic scattering (QES) at temperatures far above T_g. This contribution to the low-frequency spectrum corresponds to semi external or semi internal motions of a group of atoms or the whole molecule independently of the neighboring molecules. By contrast to the vibrational contribution, the QES corresponds to thermally activated motions and contains no structural information. Vibrational motions in the low-frequency region (ω < 200 cm^{-1}) in organic molecular materials are inherent to atom-atom potential (Lennard-Jones potential or Van der Waals interactions) mostly between the first neighboring molecules. Vibrational motions give to the low-frequency spectrum a contribution corresponding to a broad hump in disordered materials distinctive of the molecular packing (the short-range order) which is generally the rough envelop of the phonon peaks (lattice modes) distinctive of the long-range order in the crystalline state. Consequently, the information contained in the vibrational contribution is similar in the various physical states (liquid, amorphous solid, crystalline) of a molecular material, the shape of the low-frequency vibrational spectrum depending on the structural organization. It was previously shown[22] that this low-frequency region is very sensitive to the detection of the first traces of crystallization, and can be used to accurately determine the degree of crystallization from the earliest stages of recrystallization along a devitrification process. The estimate of the crystalline fraction will be obtained by determining the contribution of the lattice mode spectrum to the spectrum of partially crystallized material. The analysis of the vibrational spectrum of amorphous or partially crystallized states requires separating the QES from the vibrational spectrum.

Consequently, in a second step, the QES and vibrational components are separated by using a fitting procedure illustrated in Figure 4b, where the QES component is described by a Lorentzian shape centered at zero. After subtracting the QES from the $I_r(\omega)$-spectrum, the reduced intensity can be converted into Raman susceptibility[25] according to:

$$\chi''(\omega) = \omega . I_r(\omega) = \frac{C(\omega)}{\omega} G(\omega) \qquad (2)$$

$\chi''(\omega)$ is recognized to be a representation very close to the vibrational density of states (VDOS, $G(\omega)$)[23,26] and to provide the vibrational signature of the structural organization in the amorphous state. Figure 4c shows the $\chi''(\omega)$ spectrum of amorphous paracetamol compared

to that of the crystalline form I. They will be used in the next section to determine the evolution of the structural composition of a MCD in the course of a heating treatment.

The inset in Figure 4a shows the weak intensity of PVP spectrum compared to the spectrum of amorphous paracetamol. This is mainly due to the high content of π bonds in paracetamol with respect to PVP, that enhances the Raman signal. As a result, PVP has a very weak contribution to the overall Raman spectrum of the MCD and will be neglected in the following.

(ii) LFRS analyzes of Molecular and Crystalline Dispersions (MCD)

The MCD was heated at various temperatures (100, 110, 120, 130, 140, 150, 160 and 165°C) and the LFRS were collected at each temperature after a period of 1 hour aging. Some of them are plotted in Figure 5. It is clearly observed that only crystalline signatures (phonon peaks) corresponding to the commercial form (I) of paracetamol are detected. It can also be observed that increasing the temperature of the MCD induces a decrease of the phonon peak intensity and a broadening of the phonon peaks well observed at 165°C. These evolutions reveal the dissolution of crystalline paracetamol into PVP. For each spectrum corresponding to the molecular dispersion heated at temperatures between 100 and 165°C the same data processing was applied for determining the crystalline fraction, as described below for the MCD heated at 120°C.

In a first step the spectra of the amorphous and crystalline states were collected at temperatures at which the MCD was analyzed. $\chi"(\omega)$ of amorphous paracetamol and MCD are obtained after subtracting the QES component as described in the section 3.2.i. The integrated intensity of collective motions is the same in the amorphous and crystalline states. Consequently, all $\chi"(\omega)$ spectra were normalized in the low-frequency region where the lattice modes are detected, i.e. in the 5 – 180 cm^{-1} spectral range. The spectrum of the MCD collected at 120°C is compared to those of the crystalline I phase and the amorphous state of paracetamol at the same temperature in figure 6a. A linear combination of spectra of amorphous and crystalline states was fitted to the experimental spectrum of the MCD according to:

$$\chi"_{DMC}(\omega) = A.\chi"_{amorp}(\omega) + B.\chi"_{cryst}(\omega) \qquad (3)$$

using a least square refinement method. A and B parameters provide the contribution of the amorphous and crystalline spectra to the spectrum of the MCD. The best fit is shown in figure 6b. A good visual agreement is obtained between the experimental spectrum of the MCD and the linear combination of the crystalline and amorphous spectra of pure paracetamol, confirmed by the high value of the R factor (R = 0.9986). Given that the spectrum of PVP has a very weak contribution to the spectrum of the MCD, B closely corresponds to the fraction of

paracetamol which is in the crystalline state and A to the fraction of paracetamol which is dissolved in PVP. The solubility of paracetamol in PVP is then directly given by:

$$Solubility = \frac{A.X_{para}}{(A.X_{para})+(1-X_{para})} \qquad (4)$$

where X_{para} = 0.85 is the fraction of paracetamol in the MCD. The evolution of the solubility with the annealing temperature T_a is reported in Figure 3. It appears clearly to be coherent with the solubility line derived from the DSC investigations. This compatibility thus validates the present method of determination of solubility curves combining the use of LFRS and MCD.

4. CONCLUSION

The present study shows the capabilities of LFRS for identifying and quantitatively determining crystalline polymorph, directly and rapidly within solid dispersions. It is now recognized that LFRS can be used for the polymorph characterization of APIs[27,28]. We have previously developed a direct method based on LFRS measurements providing very fast and accurate quantification of crystalline fraction along isothermal and non-isothermal devitrification processes[22,29]. It was shown that applying LFRS for determining a crystalline fraction of drug dissolved in the polymeric matrix provides two main advantages in comparison with the use of DSC. First, this method avoids the preliminary determination of the Tg line of the drug / polymer mixture. Second, LFRS measures the solubility directly at the annealing temperature. This direct measurement is a great advantage over "scanning" methods which cannot guaranty the maintenance of this equilibrium state at temperatures below T_a. Given that the low-frequency domain becomes now accessible with routine spectrometers from the development of ultra-narrow band notch filter technology with holographic gratings[30], LFRS can be considered as a promising tool for determining solubility curves.

4. ACKNOWLEDGEMENTS

This project has received funding from the Interreg 2 Seas programme 2014-2020 co-funded by the European Regional Development Fund under subsidy contract 2S01-059_IMODE

CAPTIONS

Figure 1: X-ray diffraction patterns of paracetamol / PVP [85:15] mixture recorded at RT:
- physical mixture (black line)
- physical mixture cryo-milled for 1 hour (green line)
- physical mixture cryo-milled for 1 hour, annealed for two hours at 20°C under a plasticizing ethanol atmosphere and then dried at 80°C for 1 hour (red line)

Figure 2: Thermal protocol used to reach equilibrium saturated states at different annealing temperatures T_a.

Figure 3: In black: Evolution of the glass transition temperature (Tg) of paracetamol / PVP glass solutions with composition. The dots correspond to DSC measurements and the line represents the best fit of the Gordon Taylor law to the experimental data.
In blue: Temperature evolution of the solubility of paracetamol in PVP derived from DSC measurements. The dashed line is a guide for eyes.
In red: Temperature evolution of the solubility of paracetamol in PVP derived from Raman (LFRS) measurements.

Figure 4: Panel of low-frequency Raman spectra of amorphous paracetamol obtained by melt quenching.
a) Reduced intensity recorded at 120°C (undercooled liquid) and at -20°C (glassy state). The inset compares the Raman spectra of amorphous paracetamol and amorphous PVP recorded at -20°C.
b) Description of the fitting procedure used to separate the QES and vibrational contributions for a Raman spectrum recorded at 120°C.
c) Comparison of Raman susceptibility of amorphous and crystalline (form I) states at 120°C. These spectra were used to determine the crystalline fraction in the MCD.

Figure 5: Low-frequency spectra (Raman susceptibility) of the MCD collected after 1 hour annealing at various temperatures ranging from 120°C to 165°C.

Figure 6: Raman susceptibility of the MCD determined at 120°C (red dots)
a) compared with the Raman susceptibility of amorphous (green line) and crystalline (blue line) paracetamol determined at the same temperature (120°C).
b) compared with the best fit (black line) of a linear combination of the Raman susceptibility of amorphous and crystalline paracetamol.

REFERENCES

1. Davis M, Walker G 2018. Recent strategies in spray drying for the enhanced bioavailability of poorly water-soluble drugs. Journal of Controlled Release 269:110-127.
2. Vasconcelos T, Sarmento B, Costa P 2007. Solid dispersions as strategy to improve oral bioavailability of poor water soluble drugs. Drug Discovery Today 12(23-24):1068-1075.
3. Thakuria R, Delori A, Jones W, Lipert MP, Roy L, Rodríguez-Hornedo N 2013. Pharmaceutical cocrystals and poorly soluble drugs. International-journal-of-pharmaceutics 453(1):101-125.
4. Serajuddin ATM 1999. Solid dispersion of poorly water-soluble drugs: Early promises, subsequent problems, and recent breakthroughs. Journal of Pharmaceutical Sciences 88(10):1058-1066.
5. Jaskirat S, Manpreet W, Harikumar SL 2013. Solubility enhancement by solid dispersion method: a review. Journal of Drug Delivery & Therapeutics 3(5):148-155.
6. Dedroog S, Huygens C, Van den Mooter G 2019. Chemically identical but physically different: A comparison of spray drying, hot melt extrusion and cryo-milling for the formulation of high drug loaded amorphous solid dispersions of naproxen. European Journal of Pharmaceutics and Biopharmaceutics 135:1-12.
7. Hancock BC, Parks M 2000. What is the true solubility advantage for amorphous pharmaceuticals? Pharmaceutical Research 17(4):397-404.
8. Murdande SB, Pikal MJ, Shanker RM, Bogner RH 2010. Solubility advantage of amorphous pharmaceuticals: I. A thermodynamic analysis. Journal of Pharmaceutical Sciences 99(3):1254-1264.
9. Craig DQM, Royall PG, Kett VL, Hopton ML 1999. The relevance of the amorphous state to pharmaceutical dosage forms: glassy drugs and freeze dried systems. International-journal-of-pharmaceutics 179(2):179-207.
10. Sun Y, Zhu L, Wu T, Cai T, Gunn EM, Yu L 2012. Stability of Amorphous Pharmaceutical Solids: Crystal Growth Mechanisms and Effect of Polymer Additives. The AAPS Journal 14(3):380-388.
11. Bhattacharya S, Suryanarayanan R 2009. Local mobility in amorphous pharmaceuticals - Characterization and implications on stability. Journal of Pharmaceutical Sciences 98(9):2935-2953.
12. Graeser KA, Patterson JE, Rades T 2008. Physical stability of amorphous drugs: Evaluation of thermodynamic and kinetic parameters. Journal of Pharmacy and Pharmacology 60:116.
13. Baird JA, Taylor LS 2012. Evaluation of amorphous solid dispersion properties using thermal analysis techniques. Advanced Drug Delivery Reviews 64(5):396-421.
14. Knopp MM, Gannon N, Porsch I, Rask MB, Olesen NE, Langguth P, Holm R, Rades T 2016. A Promising New Method to Estimate Drug-Polymer Solubility at Room Temperature. Journal of Pharmaceutical Sciences 105(9):2621-2624.
15. Mahieu A, Willart J-F, Dudognon E, Danède F, Descamps M 2013. A New Protocol To Determine the Solubility of Drugs into Polymer Matrixes. Molecular Pharmaceutics 10(2):560-566.
16. Marsac PJ, Li T, Taylor LS 2009. Estimation of drug-polymer miscibility and solubility in amorphous solid dispersions using experimentally determined interaction parameters. Pharmaceutical Research 26(1):139-151.
17. Marsac PJ, Shamblin SL, Taylor LS 2006. Theoretical and practical approaches for prediction of drug-polymer miscibility and solubility. Pharmaceutical Research 23(10):2417-2426.
18. Sun Y, Tao J, Zhang GGZ, Yu L 2010. Solubilities of crystalline drugs in polymers: An improved analytical method and comparison of solubilities of indomethacin and nifedipine in PVP, PVP/VA, and PVAc. Journal of Pharmaceutical Sciences:n/a-n/a.
19. Paudel A, Van Humbeeck J, Van den Mooter G 2010. Theoretical and Experimental Investigation on the Solid Solubility and Miscibility of Naproxen in Poly(vinylpyrrolidone). Molecular Pharmaceutics 7(4):1133-1148.
20. Latreche M, Willart JF, Guerain M, Danède F, Hédoux A 2019. Interest of molecular/crystalline dispersions for the determination of solubility curves of drugs into polymers. International-journal-of-pharmaceutics 570:118626.

21. Gordon JM, Rouse GB, Gibbs JH, Risen WM, Jr. 1977. The composition dependence of glass transition properties. Journal of Chemical Physics 66(11):4971-4976.
22. Hédoux A, Paccou L, Guinet Y, Willart J-F, Descamps M 2009. Using the low-frequency Raman spectroscopy to analyze the crystallization of amorphous indomethacin. European Journal of Pharmaceutical Sciences 38(2):156-164.
23. Hédoux A 2016. Recent developments in the Raman and infrared investigations of amorphous pharmaceuticals and protein formulations: A review. Advanced Drug Delivery Reviews 100:133-146.
24. Galeener FL, Sen PN 1978. Theory for the first-order vibrational spectra of disordered solids. Physical Review B 17(4):1928-1933.
25. Shuker R, Gammon RW 1970. Raman-Scattering Selection-Rule Breaking and the Density of States in Amorphous Materials. Physical Review Letters 25(4):222-225.
26. Hédoux A, Derollez P, Guinet Y, Dianoux AJ, Descamps M 2001. Low-frequency vibrational excitations in the amorphous and crystalline states of triphenyl phosphite: A neutron and Raman scattering investigation. Physical Review B 63(14):144202.
27. Larkin PJ, Dabros M, Sarsfield B, Chan E, Carriere JT, Smith BC 2014. Polymorph Characterization of Active Pharmaceutical Ingredients (APIs) Using Low-Frequency Raman Spectroscopy. Applied Spectroscopy 68(7):758-776.
28. Inoue M, Hisada H, Koide T, Carriere J, Heyler R, Fukami T 2017. In Situ Monitoring of Crystalline Transformation of Carbamazepine Using Probe-Type Low-Frequency Raman Spectroscopy. Organic Process Research & Development 21(2):262-265.
29. Guinet Y, Paccou L, Danède F, Willart J-F, Derollez P, Hédoux A 2016. Comparison of amorphous states prepared by melt-quenching and cryomilling polymorphs of carbamazepine. International-journal-of-pharmaceutics 509(1):305-313.
30. Moser C, Havermeyer F 2009. Ultra-narrow-band tunable laserline notch filter. Applied Physics B 95(3):597-601.

Figure 1

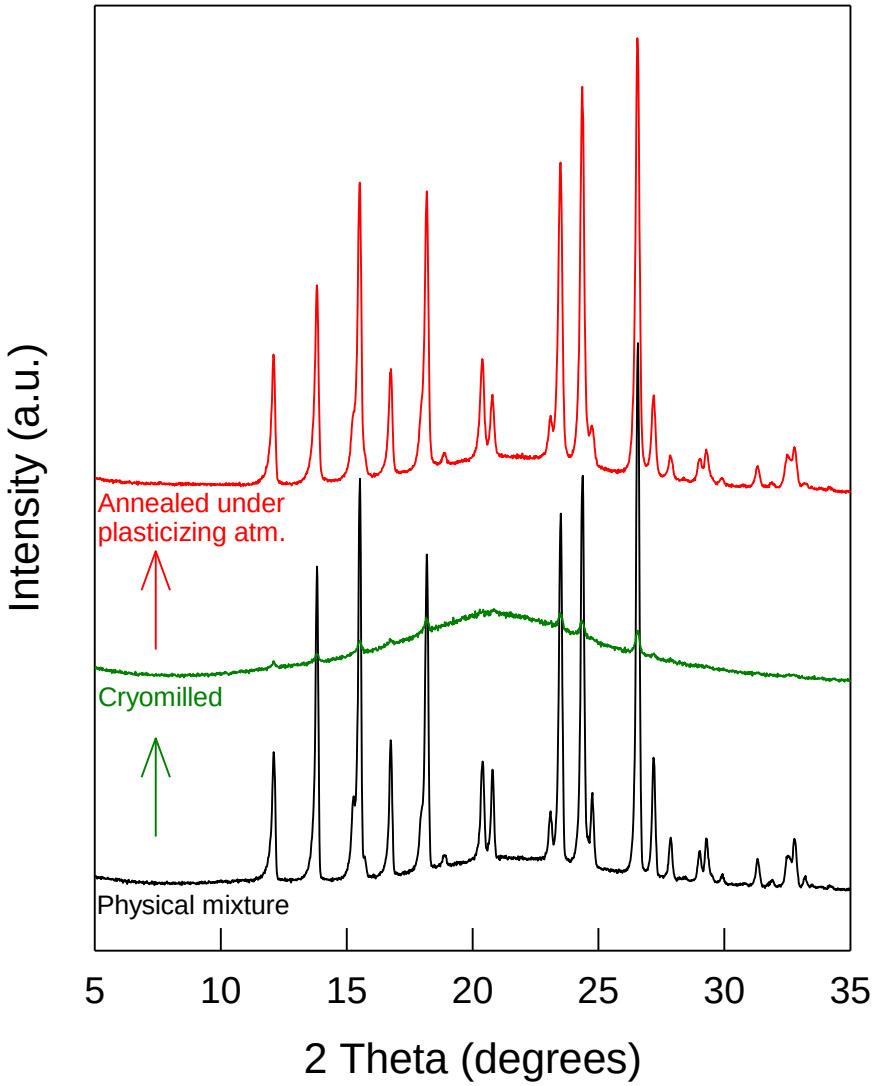
Intensity (a.u.)
Annealed under
plasticizing atm.
Cryomilled
Physical mixture
5
10
15
20
25
30
35
2 Theta (degrees)

Figure 2

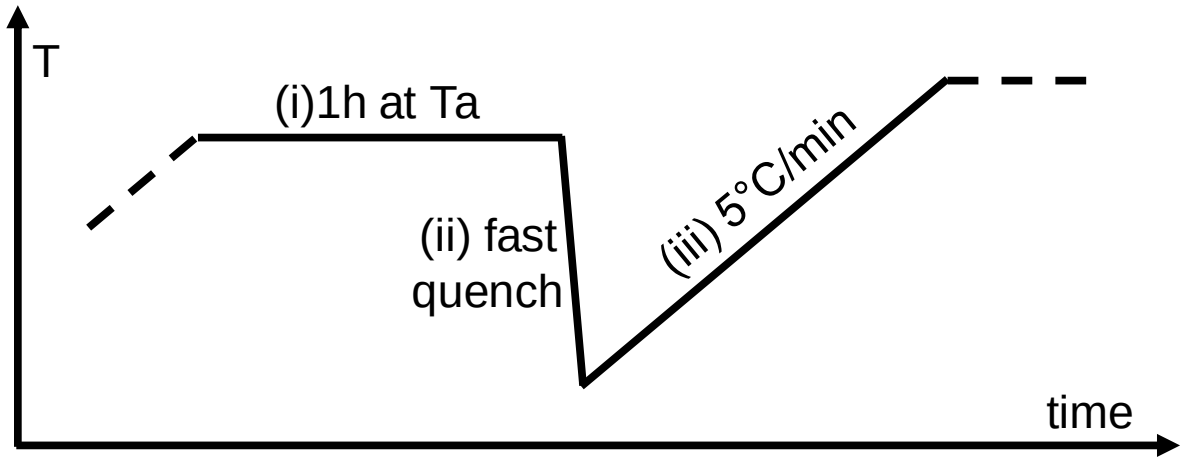

Figure 3

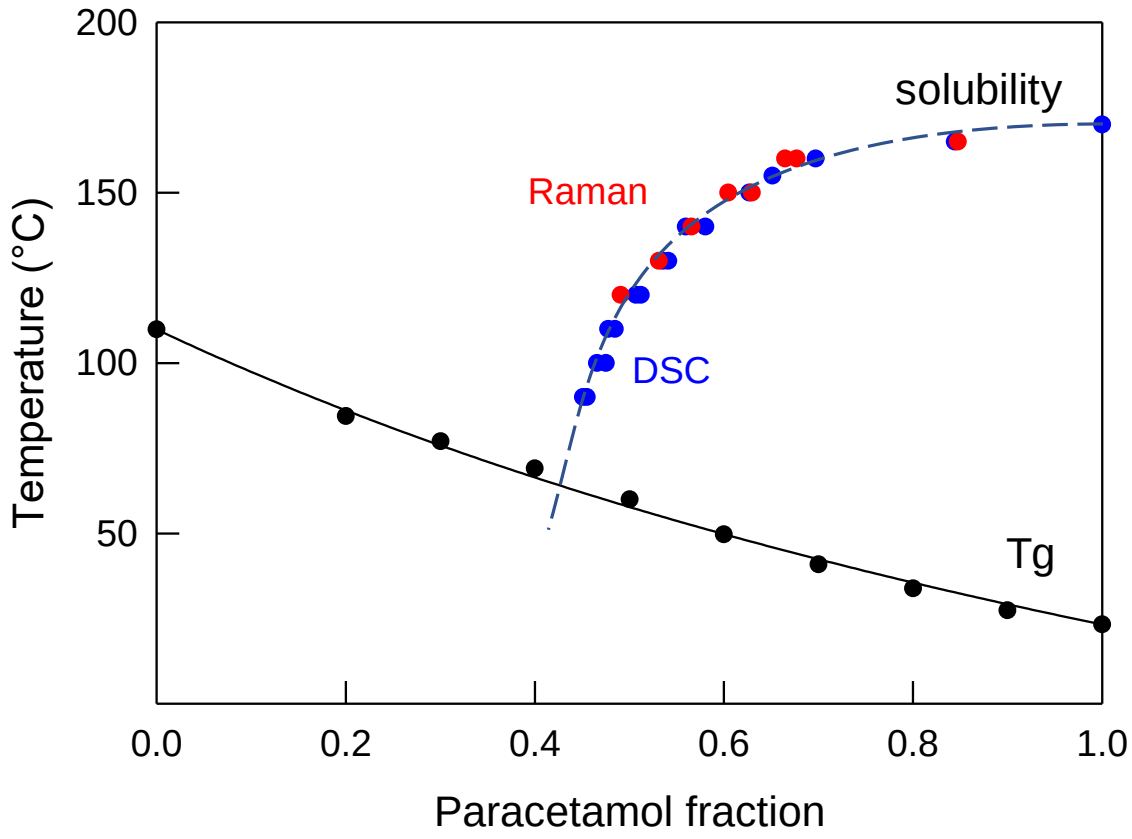
200
150
100
50
Temperature (°C)
0.0
0.2
0.4
0.6
0.8
1.0
Paracetamol fraction
solubility
Raman
DSC
Tg

Figure 4

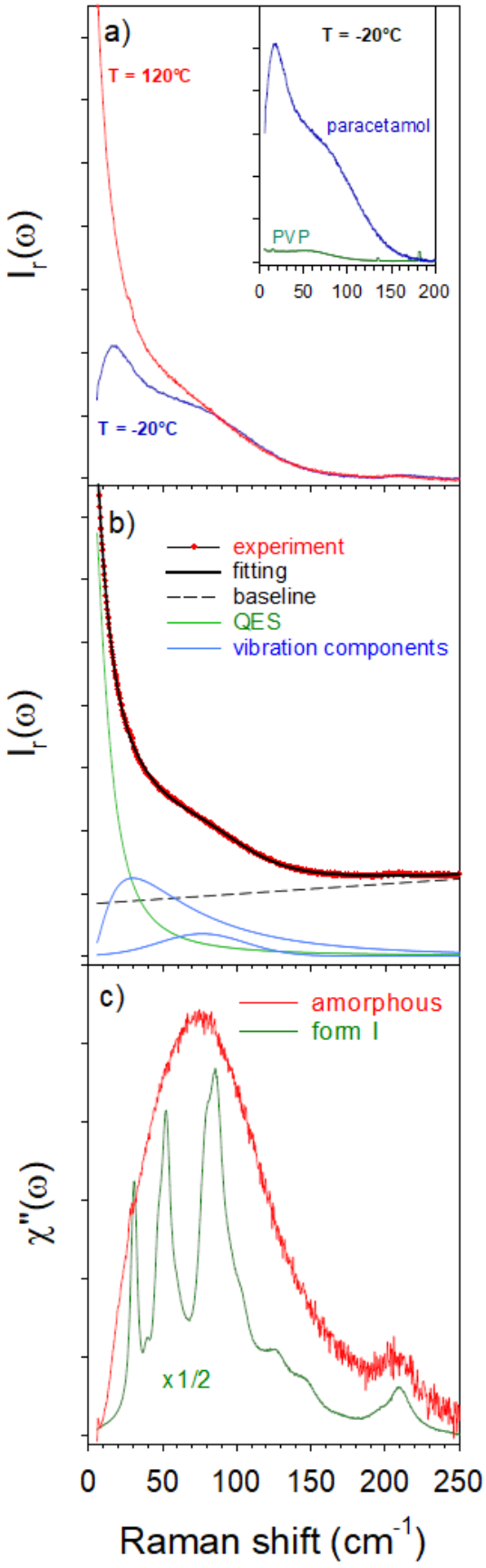
a)
T = 120°C
T = -20°C
T = -20°C
paracetamol
PVP
0
50
100
150
200
$I_r(\omega)$
b)
experiment
fitting
baseline
QES
vibration components
$I_r(\omega)$
c)
amorphous
form I
x 1/2
$\chi''(\omega)$
0
50
100
150
200
250
Raman shift (cm^{-1})

Figure 5

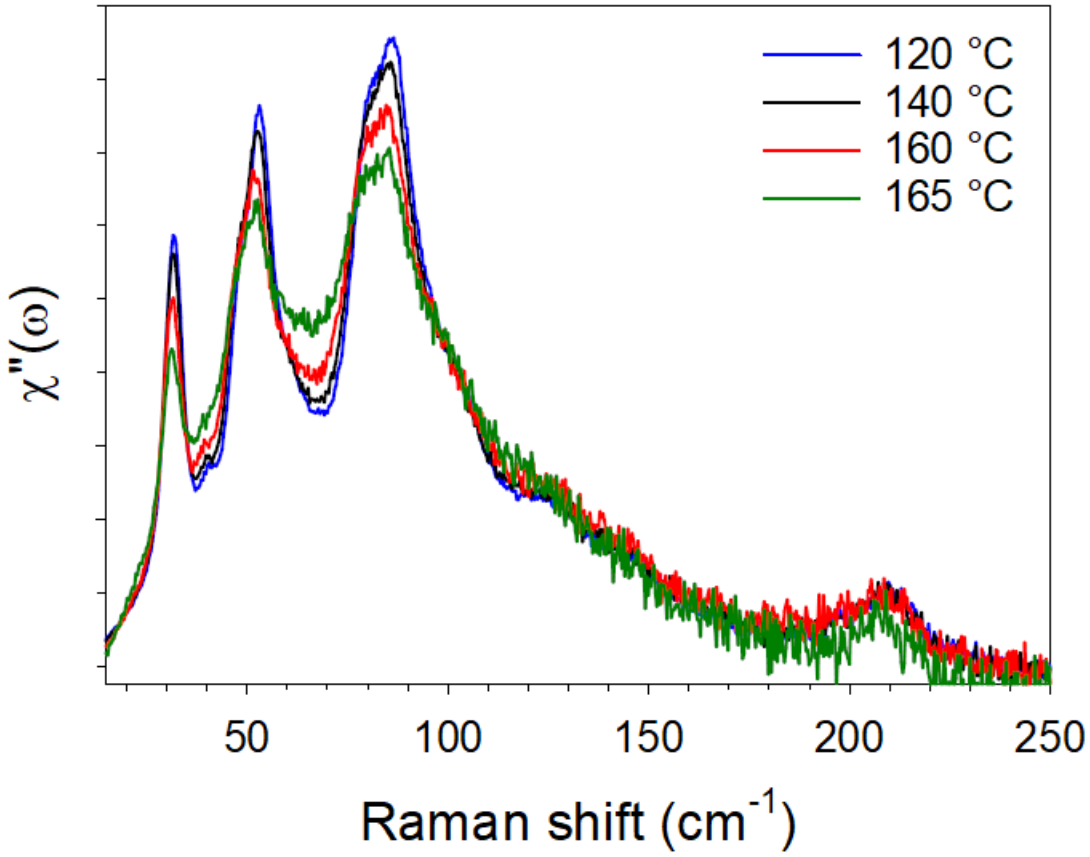

Figure 6

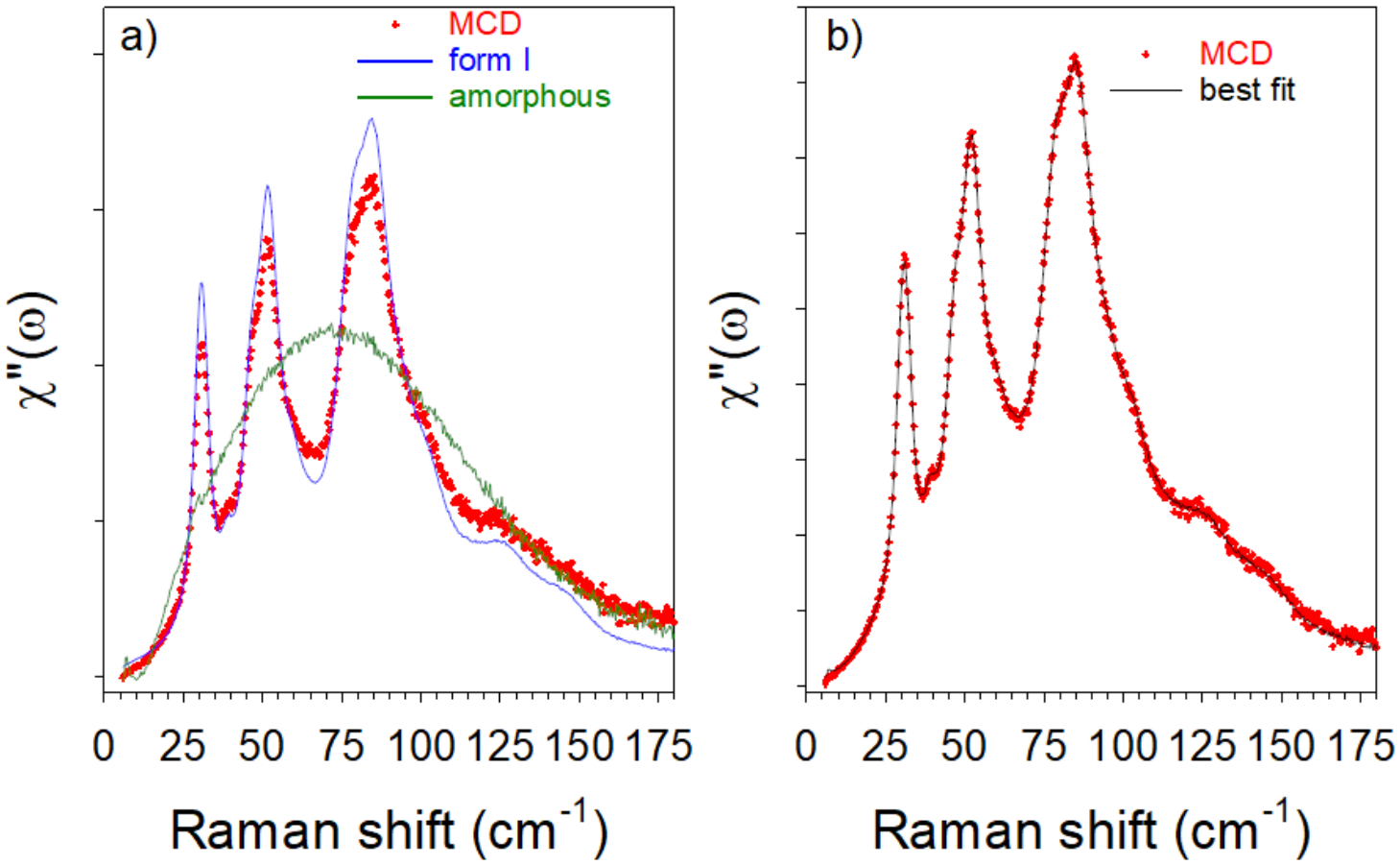
a)
MCD
form I
amorphous
χ"(ω)
0 25 50 75 100 125 150 175
Raman shift (cm-1)
b)
MCD
best fit
χ"(ω)
0 25 50 75 100 125 150 175
Raman shift (cm-1)

Graphical abstract